

Article

Are Large Particles of Iron Detrimental to Properties of Powder Metallurgy Steels?

Ahmed Abdallah ^{1,*}, Mahdi Habibnejad-Korayem ^{2,†} and Dmitri V. Malakhov ³ ¹ Department of material science, Technical Research Center, Cairo 11765, Egypt² Advanced Engineering, Stackpole International, Johnson Electric, Ancaster, ON L9G 4V5, Canada; mahdi.habibnejad@ge.com³ Department of material science and engineering, McMaster University, Hamilton, ON L8S 4L7, Canada; malakhov@mcmaster.ca

* Correspondence: asabdallah75@yahoo.com; Tel.: +2-010-6003-0474

† Current address: Advanced powder and coating, Additive Manufacturing, General Electric, Montreal, QC J7R 0L5, Canada.

Received: 5 March 2020; Accepted: 22 March 2020; Published: 25 March 2020



Abstract: It is experimentally shown that a removal of particles exceeding 100 microns in size from iron powders typically used in the fabrication of medium density powder metallurgy steels has a weak effect on apparent density, flowability and compressibility of blends as well as on density and strength of green bodies. An elimination of such particles, i.e., cutting off a heavy tail of a size distribution histogram at the 100 μm threshold, improves a compositional uniformity of sintered materials, but has no noticeable beneficial effect upon the strength of a final product, which is likely be determined by a fraction of pores and their shapes. A presence of soft pearlitic inclusions hardly matters unless their number density becomes so large that a 3D continuity (integrity) of a hard martensitic matrix is lost. This finding suggests that such an expensive preparatory step as sieving away large particles from as-received mixtures would bear no technological advantages. It was experimentally found that an attempt to lower the threshold below 100 μm noticeably worsened apparent density, flowability and compressibility.

Keywords: powder metallurgy steel; iron powder; particle size distribution; compressibility; flowability; apparent density

1. Introduction

An overall chemical composition of a typical wrought steel is a characteristic that does not deserve an elaboration, because such a steel is deemed to be compositionally uniform. Certainly, this uniformity is not observed in large billets resulting from solidification during which alloying additions are accumulating in interdendritic spaces and then along grain boundaries of a fully solidified body. However, these huge blocks invariably undergo an extensive thermo-mechanical processing during which compositional modulations inherited from casting are eliminated or at least significantly lessened. It is worth accentuating that the compositional uniformity does not imply that steel is a single-phase material. It may contain carbonitrides, manganese sulfide, oxides and other inclusions with compositions quite different from that of a ferrous matrix. If these secondary phases are finely dispersed, then any mesoscopic (but not microscopic) volumes arbitrarily chosen within a piece of wrought steel will have indistinguishable overall chemical compositions. An absence of concentration gradients in the ferrous matrix means that a change of the percentage of a solute will have a non-discriminatory spatial effect, i.e., that every mesoscopic volume will be affected in the same way. Consequently, it can be claimed that in the case of wrought steels, atoms of alloying elements are

used with an intended purpose everywhere within the material. In particular, the hardenability is a property characterizing the whole body of steel rather than its different parts. Such a remarkable and useful feature of wrought steels can partially be attributed to the fact that solutes were brought into play as individual atoms randomly distributed in liquid steel prior to casting.

In the case of steels fabricated via powder metallurgy (Let us name such steels powder metallurgy steels and use the abbreviation PMS for them), a situation may be different. Since powder metallurgy steels (PMS) is a vast realm, let us specify a kind of material this investigation is revolving around before discussing the differences.

- Compression is a single-stage process carried out at room temperature. Specifically, neither hot nor warm isostatic compaction is employed.
- It is not intended to fabricate a ferrous material with a small fraction of non-interconnected pores; post-sintering density around 7.0 g/cm^3 approximately corresponding to the fraction of pores equal to 0.1 is acceptable.
- After sintering, a final part is solutionized and quenched with an intent to produce a fully martensitic structure, which is then held at temperature, which is sufficient to relieve internal stresses, but not high enough to trigger a decomposition of martensite into ferrite and carbides.
- A characteristic size of the final part (such as the thickness of a plate) is less than an ideal diameter calculated for quenching to fully martensitic microstructure for the given overall composition.
- Iron with insignificant percentages of inevitable impurities instead of deliberately pre-alloyed iron powders is used in the process.
- Metallic alloying additions are brought into a blend as tiny particles of either individual elements or master alloys. These particles are much smaller in comparison with Fe particles.
- Carbon is brought into a mixture as a submicron graphite powder. A duration and temperature of sintering are such that a uniform carbon concentration is guaranteed.

A size distribution of iron particles is thought to be so important that it deserves a focused discussion instead of being merely a numbered item in the list above. Let us imagine a company producing PMS. It receives Fe powders from one or several manufacturers. Each batch comes with a certificate, in which, among other things such as the chemical composition, a size distribution is given. The size distribution is not prescribed by the company, because it is not clear what the optimal distribution should be. Consequently, the presence of the certificate is noticed and appreciated, but information on size distribution it contains is either given a cursory look or even ignored. Although such an attitude towards as-received powders is economically feasible, it is questionable regarding the quality of parts made of PMS. If a fraction of large particles in an as-received iron powder is significant, then they may not be properly alloyed during sintering. As a result, such particles have a reduced hardenability, which may manifest itself during quenching. Instead of being fully martensitic, a quenched part may contain soft pearlitic islands surrounded by an ocean of hard martensite. Both a fraction of pearlite and a number density of soft globules depend on the size distribution. If a corresponding histogram has a heavy right tail, then these quantities may be quite significant, and an existence of numerous soft inclusions may detrimentally affect mechanical properties. However, a possible worsening of mechanical properties due to pearlitic inclusions is a conjecture at best, because an influence of inevitable pores in PMS may have a much greater effect.

If it is established that the presence of underalloyed particles is adverse, then the company can either sieve them away or, better, try to identify a manufacturer capable of producing Fe powders in which particle size does not exceed a certain threshold. Let us admit that getting rid of a heavy right tail of the histogram is not as daunting a task as making a powder with a predetermined size distribution. If, on the other hand, it is found that the existence of soft island is immaterial, then no actions are warranted, and the company making PMS products should not consider changing a manufacturing routine already in place.

An ability to yield a compositionally uniform sintered material at the end of a technological chain is not the only characteristic of an iron powder, which ought to be taken into account. As shown in the next section, a removal of large particles may lead to degrading apparent density, flowability and compressibility. Obviously, the problem is multifaceted, and its complexity suggests that serious experimental efforts are required to either ascertain the threshold mentioned above or show that it does not exist.

2. Literature Review

The manufacturing of materials by means of powder metallurgy (PM) is influenced by the characteristics of starting powder. The most relevant characteristics are particle size distribution, particle shape, impurity level and surface characteristics [1]. Properties such as apparent density, flowability and compressibility depend on the characteristics of initial powders. Properties of green compacts such as porosity, roughness and green strength depend on initial powder properties as well. The same is true for the mechanical and microstructural properties of sintered products [2].

An important physical property of a fresh powder is its apparent density (AD); this characteristic is decisive in determining die dimensions. It is governed by particles shapes, size distribution, surface area per unit volume, moisture content and usage of lubricant. It has been reported that AD of powders with small particles is higher than that shown by powders with larger particles of the same material [3]. However, the opposite conclusion was also reported. Sanchez et al. [2] stated that AD diminishes when the particle size decreases due to the internal friction increase. Tikhonov et al. [4] studied the effect of particle size distribution on properties of stainless-steel powders, they reported that with a rise in amounts of fine and medium fractions in powder mixtures, AD increased. They also stated that with adding fine powder to a coarse powder, the AD may either increase or decrease. If the fine particles become distributed in the interparticle pores of a coarser fraction, the AD increases, but if it remains outside the pores, a reduction of AD occurs. Peterson et al. [5] stated that the AD decreased with narrowing the particle size distribution, and this was explained by the interaction between the large and small particles in each mixture. Additionally, they found that removing fine particles resulted in a higher decrease in AD than removing coarse ones [6].

Flowability is a vital characteristic of powders as it reflects an ability of powders for a rapid and uniform die filling. It is affected by the size distribution of particles and their shape, moisture, entrapped gases, lubricant, powder packing and interparticle friction. It was reported that small particles generated high interparticle friction that restricted powders to flow [3]. Peterson et al. [5] observed that a flow rate of iron powders increased with rising a fraction of coarse particles. Tikhonov et al. [4] stated that the flowability of a mixture of fine and coarse powders depended on packing particularities. In general, previous researches showed that the flow rate was enhanced by decreasing the particle shape irregularity [1,5].

The green strength of a compact depends on the consolidation pressure and arises mainly from cold welding and interlocking of neighboring particles. The green body strength must be such that a part can withstand an ejection from the die followed by a transfer to a sintering furnace. Many studies were carried out on metal powder green strength. A higher strength of green bodies was obtained for small-size particles, which can be explained by an increase of a number of contact points [7]. According to Sanchez et al. [8] the green strength of iron powders reaches a maximum value at intermediate particle size due to the effect of particle morphology and number of bonds. Suh et al. [9] studied the effect of particle size distribution; it was stated that two competing factors existed, namely, interparticle friction and interlocking, and that the maximum green body strength corresponded to a particular packing factor of a mixture of fine and coarse powders. Olikier [10] reported that green strength grows with decreasing particle size and increasing surface roughness.

A compaction is a crucial link in a production chain of PMS. Compressibility of powder can be affected by many factors such as spatial variations of green density [11], size distribution of particles and their shapes, specific surface area, use of lubricant, presence of impurities, powder hardness,

entrapped air and compacting technique [9]. It was stated that the use of small metallic particles caused problems during pressing due to a large specific surface area, leading to high friction between particles [2,12]. Tikhonov et al. [4] presented experimental evidences that with increasing fractions of fine and medium particles in a powder mixture, the degree of compression decreased. Sorokin [13] studied the effect of particle size distribution on compressibility, and he demonstrated that at low compaction pressures, the addition of coarse powder increased the degree of compressibility, while at higher pressures, it is independent of particle size distribution, being mainly determined by particle shape and apparent density of the powder. Suh [9] stated that iron powders with wide size distribution and irregular shape exhibited a better compressibility. A discussion focused on compressibility of powders will be incomplete without mentioning the paper by Fischmeister et al. [14] (1978 Fischmeister Arzt Olsson), in which a metallographic examination of isostatically and uniaxially compressed bronze powder revealed how a contact area and a coordination number evolved with increasing pressure. Results of mainly experimental work (1978 Fischmeister Arzt Olsson) were rationalized by Fischmeister et al. [15] (1983 Fischmeister Arzt) who identified restacking (rearrangement and sliding), densification and impingement of interparticle contacts as three distinct compaction stages. The authors derived an intricate yet beautiful equation, in which a term describing “the flow and strain hardening behavior of the particle material” is distinguished from a “purely geometrical” term, in which initial density and coordination numbers as well as information on particularities of particles packing are reflected. Although the mathematical model was developed for spheres of the same size, but moderate size and shape deviations will not nullify its practicality.

Kiparosov [16] investigated the effect of particle size of steel powders on the sintered properties. He stated that with decreasing particle size sinterability improved. Additionally, he concluded that the finer the starting powder, the lower the sintering temperature necessary for the attainment of a given density. Lund et al. [17] maintained that use of iron powders with small particle size led to enhanced mechanical properties of sintered bodies due to higher specific surface area, which increased a number of bonds among the particles. Moreover, Sanchez et al. [2] stated that increasing the powder size resulted in decreasing transverse rupture strength of sintered iron samples. The effect of particle size distribution of iron in PMS was investigated by many researchers [9,10]; they demonstrated that minimum pore size and maximum sintered strength could be obtained by utilizing mixtures of optimally packed coarse and fine particles. Tallon et al. [8] studied the effect of size distribution of iron powder on hardenability. It was found that with smaller particles of iron, sintering time could be reduced, and superior PMS could be produced. However, it was mentioned that sintering time for PMS might be insufficient for relaxation to homogeneity. For typical sintering times and temperatures, an insufficient alloying becomes a serious problem for Fe particles exceeding 150 μm . Even if a sintering time is deliberately made impractically prolonged, interiors of these large objects may remain underalloyed and therefore less hardenable. Using pre-alloyed powders (such as Fe-0.5%Mo) resolves this problem, but, in general, such mixtures made of particles less ductile than pure Fe may show poor compressibility. Interestingly, it was observed that a significant percentage of coarse Fe particles resulted in large pores. Finally, Tallon et al. observed that PMS made of fine powders had higher density, hardness and tensile strength.

The main objective of this research is to investigate the effect of particle size distribution of iron powder as a base metal in a PM steel alloy containing Cr, Ni, Mo and C on the flowability, compressibility, green and sintered properties. Additionally, as iron powders used in PMS have a wide size distribution with heavy tails, it is aimed to estimate an upper limit of cutting tail below which properties deteriorate noticeably.

3. Experimental Procedure

The experimental approach chosen in this research was straightforward and laborious. Flowability and compressibility of an as-received iron powder whose size distribution was meticulously established were measured. Then a set of sieves was used for an incremental removing of large particles. Firstly,

ones with sizes exceeding 180 μm were sieved away (the percentage of such particles in three different Fe powders employed in this investigation varied from 1.7% to 6.6%), and flowability and compressibility of a remaining powder were measured. Then another mixture, from which particles greater than 150 μm were removed, was obtained and characterized. This process of an incremental elimination was replicated until either flowability or compactability became inadmissibly poor. Once a limit below which the right tail of the size distribution should not be cut off was identified, a corresponding iron powder free of large particles was mixed with alloying additions, graphite and a lubricant. A resulting blend was then used for fabricating a PMS object whose properties were compared with another object having the same chemical composition and processed identically, but produced from an original unsieved powder.

This procedure was repeated for three batches of Fe powders obtained from different manufacturers. Instead of revealing their names, it was decided to unpretendingly designate them as A, B and C. In all three cases, a side-by-side comparison of microstructures and selected mechanical properties allowed us to make a definite conclusion regarding the role playing by large particles in PMS.

3.1. Choice of the Chemical Composition

The chemical composition of an object made of PMS must be considered in relation to its size and shape as well as to quenching conditions. Specimens used in this investigation were 12 mm \times 12 mm \times 30 mm parallelepipeds. By employing SteCal software [8], it was found that the equivalent critical diameter of an infinitely long cylinder was 8 mm. If this cylinder is quenched in a stagnant (not agitated) oil, for which the severity of quench $H = 0.3$, then SteCal can predict 36 mm as the ideal critical diameter, DI. If oil is moderately agitated (stirred), then $H = 0.3$ and $DI = 28$ mm. It is likely that quenching in forced helium at 20 atm employed in the present investigation, resembles quenching in still oil. Based on this, a composition resulting in an appropriate DI can be chosen. Of course, such a composition is not uniquely defined, and in order to proceed, a circle must be narrowed. Firstly, it suggested to use Mn-free alloys, because, according to the literature and accumulated experience, even large Fe particles are alloyed with manganese quite well [8]. Secondly, let us use Ni, which diffuses slowly. Additionally, it is sensible to consider Cr and Mo, which are customarily utilized in ferrous powder metallurgy. Finally, let us take 0.5 wt. % of carbon, which is typical for PMS. Through carrying out SteCal calculations, the chemical composition shown in Table 1 was identified.

Table 1. Chemical composition of powder metallurgy steels (PMS) used in this investigation.

Element	C	Ni	Cr	Mo	Fe
Mass %	0.5	0.5	0.8	0.2	balance

For this grade, the ideal critical diameter of a cylinder along the centerline of which the percentage of martensite was 99% was 27 mm, and for 50%, this diameter was 49 mm. In view of this, one can anticipate pearlitic globules in the interior of the 12 mm \times 12 mm \times 30 mm bars utilized in this research.

Lubricant was added (0.7 wt. %) to improve compressibility and green strength by reducing friction between powder particles, or between powder particles and die walls, which has a more pronounced effect. The prescribed chemical composition and the dimensions of the test samples were chosen, to get a multiphase alloy after heat treatment, which enables to display the effect of the removing coarse iron powder.

3.2. Characteristics of Used Powders

Three different iron powders produced through water atomization, denoted A, B and C were used as a base metal, the morphology of these powders was revealed by SEM as shown in Figure 1. It can be observed that all the types of iron powder have irregular morphology. It can partially be attributed to the agglomeration of almost spherical particles fabricated during atomization. The average particle

size of the alloying elements was much smaller than that of iron. Typically, it varied between 6 and 12 μm .

For each iron powder type, the size distribution was established according to the ASTM (standard B214-16). It is clear from the histograms in Figure 2 that none of these distributions were unimodal. It is worth mentioning that although the three powders investigated were received from different manufacturers, the size distributions were quite similar.

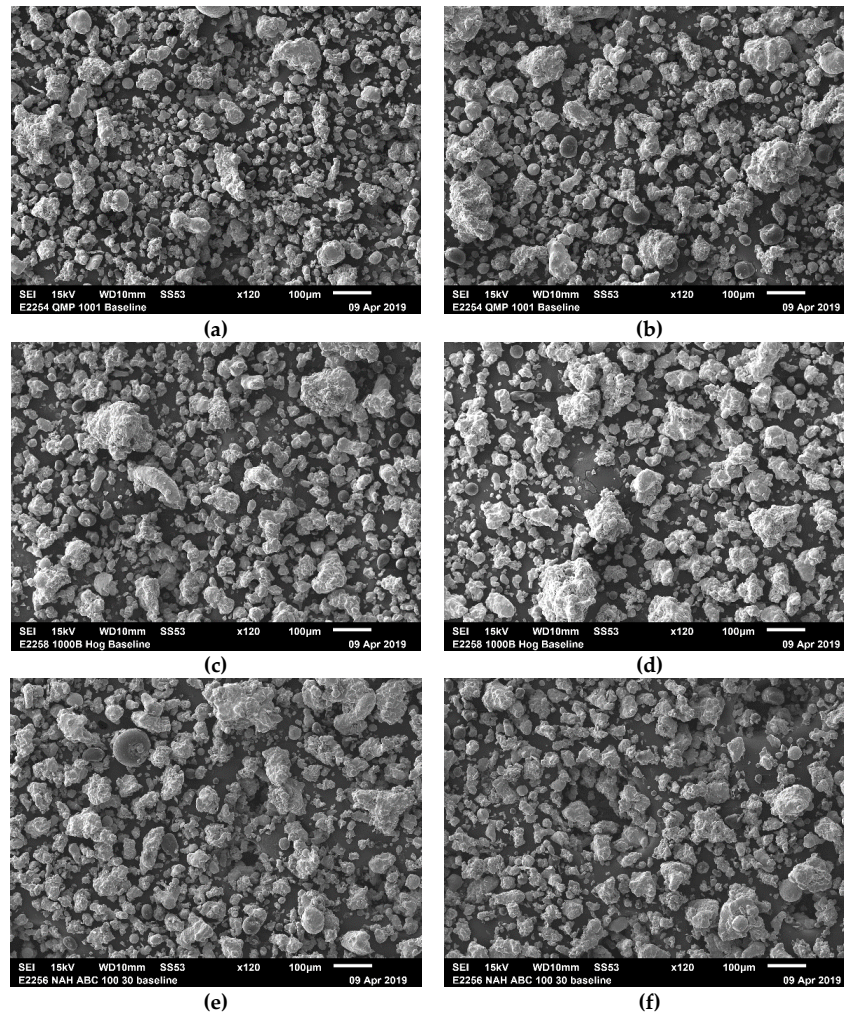


Figure 1. SEM images of as received iron powders, (a,b) are images for iron powder type A, (c,d) are images for iron powder type B and (e,f) are images for iron powder type C.

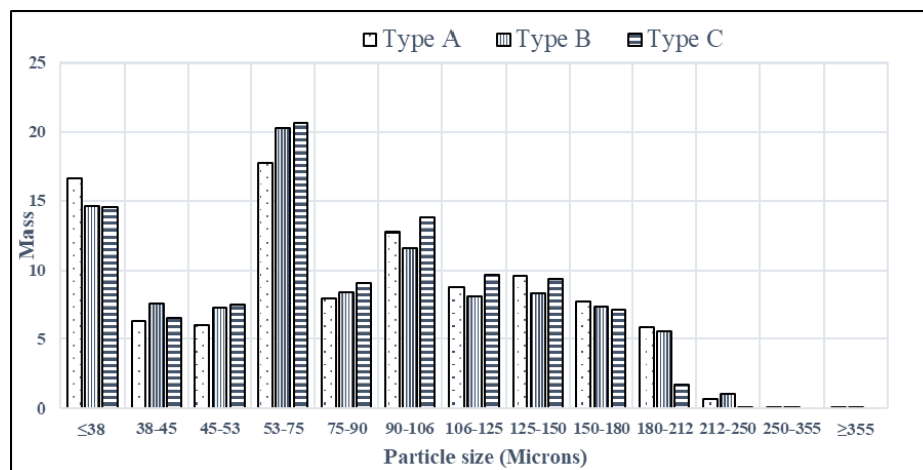


Figure 2. Particle size distribution of pure iron powder.

The apparent density of all the powders was evaluated using the Hall flowmeter funnel, according to the ASTM (standard B212-17). The flow rate for powders was determined according to the ASTM (standard B213-17); 50 g of powder was timed to flow unaided through an orifice in a calibrated Hall flowmeter funnel. Measurements of the apparent density and flowability were repeated five times to ensure the reproducibility of the results.

3.3. Compressibility Tests

A uniaxial MTS press was used to carry out compressibility tests. As both upper and lower punches move, this kind of test fell into the “double action pressing” category. Compaction was performed in air, at room temperature. At the end of each compaction, there was a 10 s dwelling mandated by the ASTM standard B331-16.

A set of preliminary experiments were performed to evaluate the effect of powder height in the die and compaction rate on the compaction process. In each set of experiments, only one variable was examined, while other experimental parameters were constant to exclude their effect. The compaction was performed using powder samples with different masses (2–2.5–3–3.5) grams using a cylindrical die with inner diameter 9.5 mm, then, the load rate was changed from 0.2 to 1 to 2 mm/min. Those preliminary trials were launched in order to find ranges of powder masses and strain rates within which density vs. pressure plots were weakly (negligibly) affected by those factors.

For the rest of compressibility tests, each specimen corresponded to 3 g of powder. A cylindrical die of inner diameter 9.5 mm was used. A colloidal suspension of 5 g of zinc stearate in 100 g of butanol was applied to a punch and die’s inner wall. After drying, they were uniformly covered with a thin zinc stearate layer. It is worth accentuating that in preliminary experiments performed with pure Fe, lubricant was not admixed; only the punch and the die were lubricated. However, all mixtures of iron with C, Cr, Ni and Mo always contained approximately 0.7 wt. % of Dura Lube polyolefin. All experiments were conducted with a constant strain rate of 1 mm/min.

After compaction, green body disks were weighted with the accuracy 0.01 g, and the dimensions were measured with the accuracy 0.01 mm. This information along with a fact that the crosshead moved with a constant velocity was used to reconstruct density vs. pressure curves. Every compaction experiment was repeated three times to ensure the reproducibility of experimental data.

3.4. Preparation of Samples

Mixtures of Fe, tiny powders of alloying additions and graphite as well as a lubricant were blended for 45 min, which is a typical duration of such a process. Then unidirectional pressing was applied for consolidation of metal powders into two groups of transverse rupture strength (TRS) bars; the

first group were standard 6 mm × 12 mm × 30 mm parallelepipeds prescribed in the ASTM standard B312-14, and the second group comprised of enlarged TRS bars with dimensions 12 mm × 12 mm × 30 mm. All the mixtures were compacted with the same load. This identical load resulted in a slight difference in the green densities of the compacts. Sintering was carried out in a belt furnace with time–temperature profile, shown in Figure 3. The initial temperature at 900 °C was the opening stack burner, followed by the preheat zone where temperatures slowly reached 775 °C. This was to burn off the lubricant within the part before sintering. The high heat zone then increased to 1280 °C for roughly 30 min in an Argon-5%Hydrogen atmosphere before slowly cooling.

After sintering, the samples were heat treated; according to the thermal cycle shown in Figure 4. There is enough time at 900 °C (75 min) to form the austenitic phase. The atmosphere is primarily nitrogen at a very low atm, to remove any residual gasses from the parts and to insure no oxidation or decarburization during the thermal treatment. The quench is completed in 12 min, using cooled helium. Tempering was conducted at temperature, which was high enough to remove internal stresses, but not to cause a transformation of martensite into ferrite and carbides.

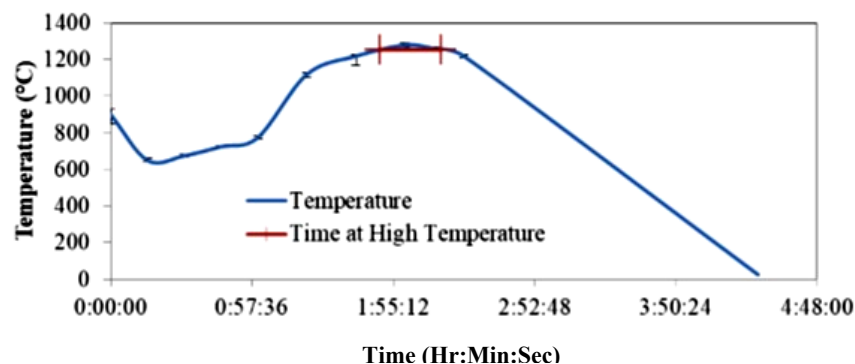


Figure 3. Sintering cycle for PM steel alloy.

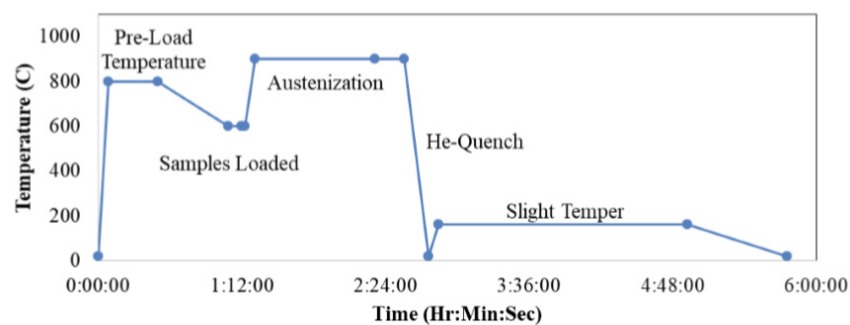


Figure 4. Heat treatment cycle for powder metallurgy (PM) steel alloy.

3.5. Characterization of Samples

Three TRS bars for each powder type were used in the green state to measure green body strength via the three-point bending test described in the ASTM standard (B312-14). Three other bars were used to measure the transverse rupture strength in the heat-treated state according to the ASTM standard (B528-16). Rockwell hardness A was measured on the surface and in the core of the bars after heat treatment. Sintered density was evaluated by the Archimedes method according to the ASTM standard (B962-17). Standard metallographic procedures were utilized for preparing specimens for optical microscopy examinations. In all cases, etching with 2% nital for two seconds was adequate to reveal the microstructure.

3.6. Sequence of the Experimental Work

In the first set of experiments, the sample mass and strain rate were determined, using iron powder type A, to be used in the compressibility evaluation experiments. A second set of experiments was performed to evaluate the apparent density, flowability and compressibility of pure iron powder. Fractions of powder were prepared from the three iron powder types, by excluding coarse particles from the original powder gradually. Studying the behavior of the powder fractions, a recommended cut off limit for each type was suggested. Then six PM steel blends were produced, with the same concentrations of carbon and metallic additions. In the first three mixtures, iron was added in the as received state, and in the other three mixtures, it was added according to the recommended particle size distribution after removing coarse particles, i.e., after cutting heavy tails of the distributions. After preparing blends, compressibility and green density for all powder mixtures were measured. In the final set of experiments, characteristics of sintered standard and enlarged transverse rupture strength samples were evaluated.

4. Results and Discussion

4.1. Compressibility of Pure Iron Powder

The green density increased slightly with increasing the powder mass, until it reached a maximum value, then it started to decrease, due to the occurrence of density gradient between the parts of the compact along the axial direction. In addition, there was a range of masses (heights) within which the green density remained almost the same, and that we operated inside this interval. A negligible increase in green density occurred with decreasing load rate. These results were consistent with previous findings regarding the effect of loading rate on the compressibility of powders [18,19].

4.2. Properties of Metal Powders

The apparent density, flowability and compressibility of pure iron and powder blends were evaluated. The results are shown as follows:

4.2.1. Size Dependent Properties of Pure Iron Powder

Apparent Density

Apparent density measurements were performed for all three pure iron as-received batches without lubricant as well as for powders, from which, coarse particles were incrementally sieved away. It was believed that shifts in the particle size distribution towards smaller particle sizes would increase the apparent density of the powder, while shifts to larger sizes would decrease this property. However, the measured apparent density values did not confirm these predictions. It was found that, with removing coarse particles and narrowing the particle size distribution, the apparent density decreased as shown in Figure 5.

This may be explained by considering the packing of large and small particles. As small particles fill not only the pores between larger particles but also the caverns between those irregular particles in the as received state. This packing increased the mass without increasing the volume, which increased the density of the original powder. Removing the coarse particles gradually decreased the apparent density, as smaller particles would occupy the volume vacated by the removed large ones leading to porous packing, which lowered the mass and increased the volume. This phenomenon was observed earlier by Peterson et al. [6], they stated that the interaction between the large and small particles is critical to the apparent density. Additionally, the removal of coarse particles caused a pronounced decline in this property.

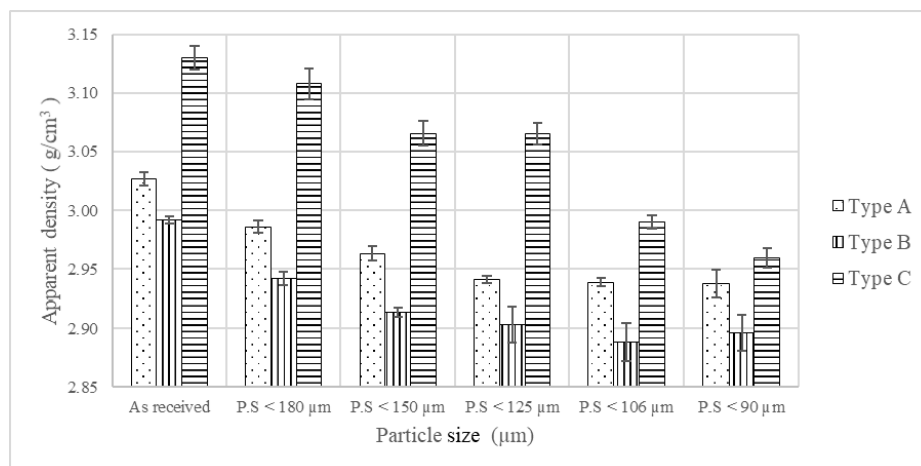


Figure 5. An influence of an incremental cutting-off a heavy tail of the size distribution on the apparent density of pure iron. The notation P.S. < a μm means that all particles with sizes greater than a μm were removed.

Flowability

The flow rate for all pure iron powder types without lubricant, in the as received state, and after removing coarse particles with sizes exceeding 180, 150, 125, 106 and 90 microns respectively, was measured. In general, flow time shortened for all iron powder types with removing coarse particles. As Figure 6 suggests, an extent to which this decrease was noticeable, differed from one type of powder to another.

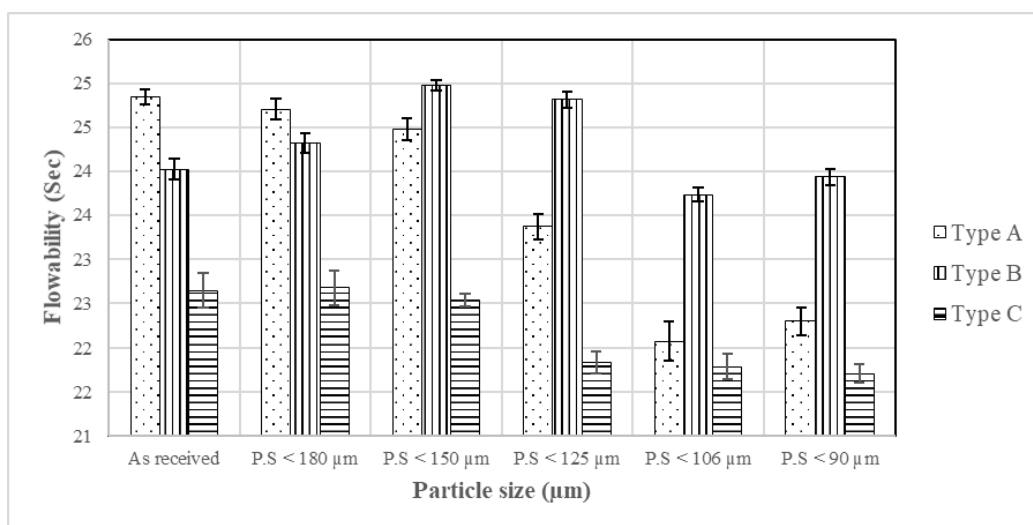


Figure 6. Flowability of pure iron powder, in the as received state, and after removing coarse particles with sizes exceeding 180, 150, 125, 106 and 90 microns respectively.

This effect can be related to increasing the homogeneity of the powder with removing coarse particles, leading to better flowability. In addition, as the size of particles become smaller, their shape gradually becomes more spherical. So, particles will have fewer point contacts and face little interparticle friction to hinder flow. This explanation was verified by Peterson et al. [5], who stated that the removal of coarse irregular particles has a pronounced effect on the flow time of iron powder.

Compressibility

The compaction response of different types of pure iron powders without lubricant shows the same behavior, which can be divided into three different stages, visible in Figure 7. At the beginning of the compaction cycle, the powder had a density approximately equal to the apparent density, and even with vibration, the highest obtainable density was only the tap density. As pressure was applied, the first response was the rearrangement of particles with the filling of large pores. During this stage geometrical factors contributed the most [11], and densification increased suddenly. Increasing pressure led to decreasing porosity with the formation of new particle contacts. The contacts underwent elastic deformation, which is totally reversible. Higher compaction pressures increased density by contact enlargement through plastic deformation, along with a decrease in the densification rate. Plastic deformation was first localized at the contact areas between particles, and as the pressure increased, homogeneous plastic flow spread from the contacts and the entire particle became work hardened [20]. Both the elastic deformation and work hardening were related to the microstructure of the powder [11].

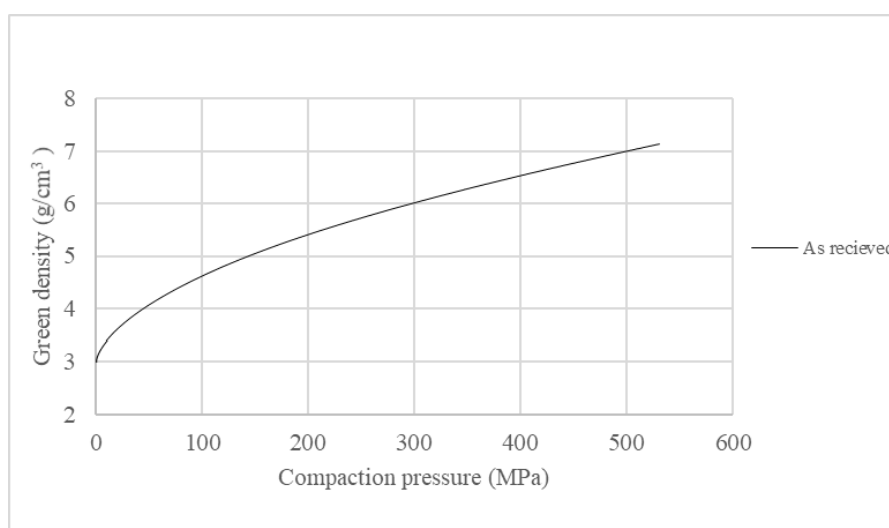


Figure 7. Compressibility evaluation for pure iron powder type A, without adding a lubricant, in the as received state.

Compressibilities of different as received types of pure iron powders without a lubricant, and those from which coarse particles were incrementally removed, are shown in Figure 8. Compressibility gradually decreased with excluding coarse particles gradually, in all iron powder types. This can be illustrated by increasing the portion of fine particles, which have a higher specific surface area, leading to higher friction and higher-pressure losses during pressing. In addition, coarse particles have less contact surfaces than smaller ones, so, less interparticle friction dominated in the first case, and this improved particle mobility and packing during compaction.

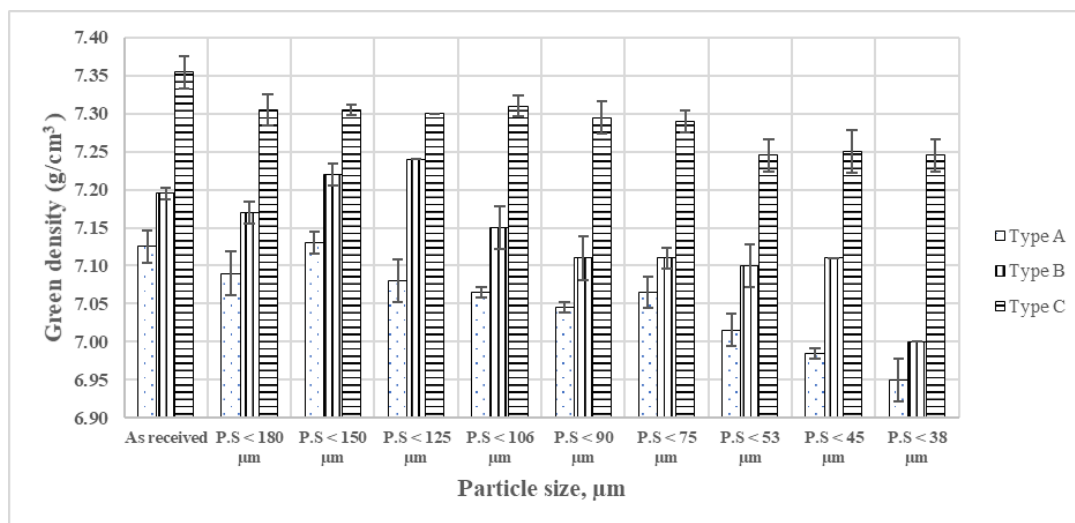


Figure 8. Densities of pure iron powder without adding lubricant, after achieving the terminal load of 49 KN. The notation P.S. < a μm means that all particles with sizes greater than a μm were removed.

A critical analysis of experimental data on flowability, apparent density and compressibility led to a conclusion that in order to maintain these characteristics at acceptable levels, a removal of coarse particles must stop at the following thresholds: 90 μm for type A, 106 μm for type B and 90 μm for type C. It can be hypothesized and hoped that an elimination of coarse particles will facilitate an attainment of flat concentration profiles of Mo, Cr and Ni resulting in a spatially uniform hardenability of PMS, which will manifest itself in an absence of large and soft pearlitic islands in the interior of the material.

4.2.2. Size Dependent Properties of Blends

Powder blends containing pure iron, carbon, lubricant and other alloying additions were prepared according to the prescribed chemical composition. The powder mixtures A', B' and C' are powder metallurgy steel mixtures, where pure iron powder types A, B and C were added in the as received state respectively. While; A'90, B'106 and C'90 are mixtures, where same iron powder types were added after removing particles bigger than 90, 106 and 90 microns respectively.

Constant-Load-Green Body Densities

All powder mixtures were pressed to form standard transverse rupture strength samples. It was found that no significant change in the green density for powder mixtures prepared with as received iron powder and sieved iron powder after removing coarse particles, as shown in Figure 9.

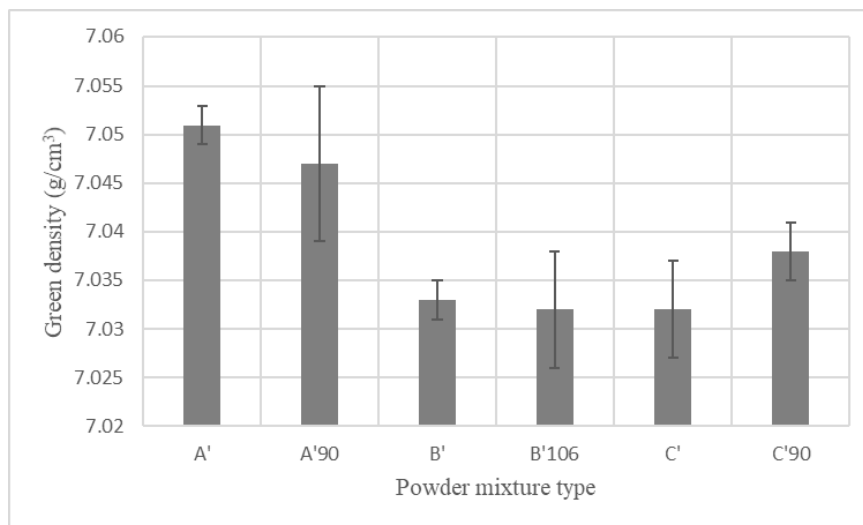


Figure 9. Compressibility evaluation for PMS mixtures (including 0.7 wt. % of the lubricant).

4.3. Green Body Strength

The strength of green bodies for compacts prepared from mixtures where iron powder was added in the as-received state, was observed to be significantly higher than that of compacts with sieved iron powder after removing coarse particles, as shown in Figure 10.

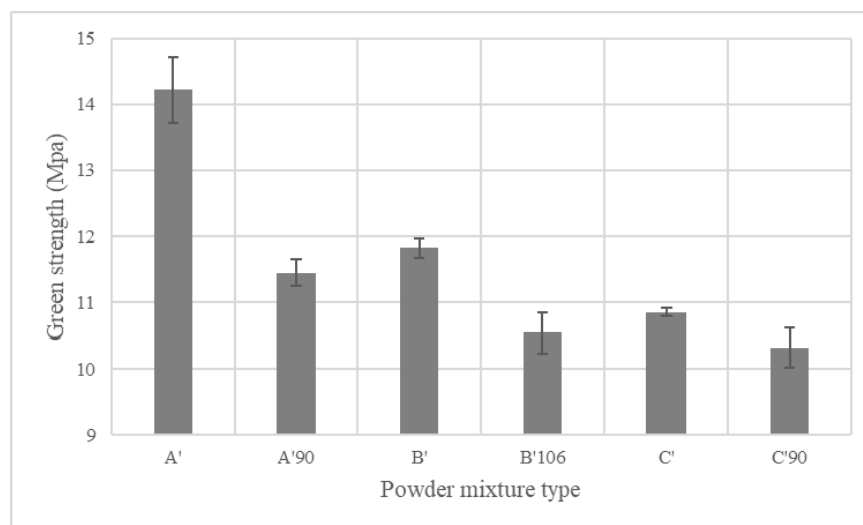


Figure 10. Green strength for various PMS mixtures (including 0.7 wt. % of the lubricant).

The higher green strength for mixtures with as received powder could be due to better packing between fine and coarse powders, in which fine particles filled voids between large ones, leading to higher interlocking of particles.

4.4. Sintered PMS Alloy Properties

The effect of removing coarse iron particles on the physical, mechanical and microstructural properties of the steel alloy in the sintered and heat treated state is characterized in terms of sintered density, hardness and transverse rupture strength. Microstructure variations, notably the martensite formation was observed at the surface and the core of all samples.

4.4.1. Sintered Density

Results of sintered density measurements, for specimens in the sintered and heat treated state, show an insignificant influence with removing coarse iron particles from the powder mixtures, as shown in Figure 11.

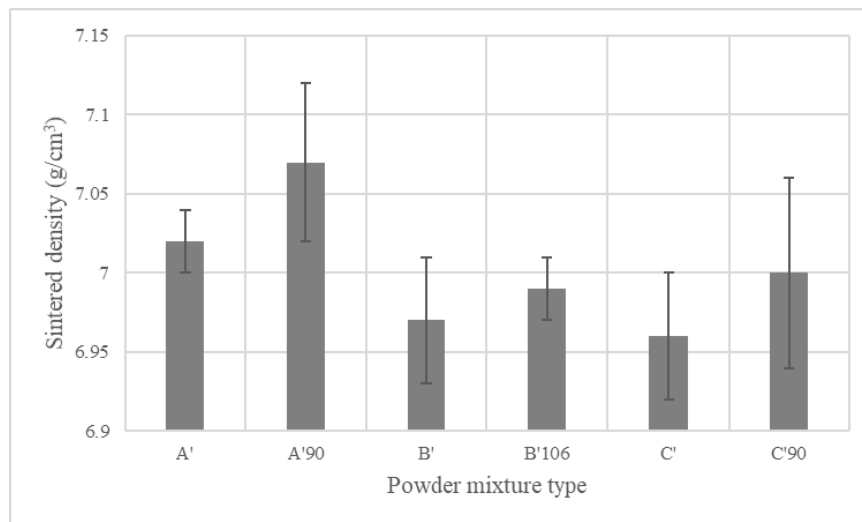


Figure 11. Density of standard transverse rupture strength (TRS) samples prepared from various PMS mixtures (including 0.7 wt. % of a lubricant).

4.4.2. Optical Microscopy

The steel was austenitized at 900 °C and quenched in helium to form martensite. The micrograph shown in Figure 12 was for a sample prepared using as received iron powder type A. The microstructure revealed parallel narrow lathes of martensite (gray areas), low carbon martensite (white areas) formed due to inhomogeneity of the structure, and different scattered islands of pearlite (dark areas) formed with different densities from the core to the surface corresponding to the cooling rate.

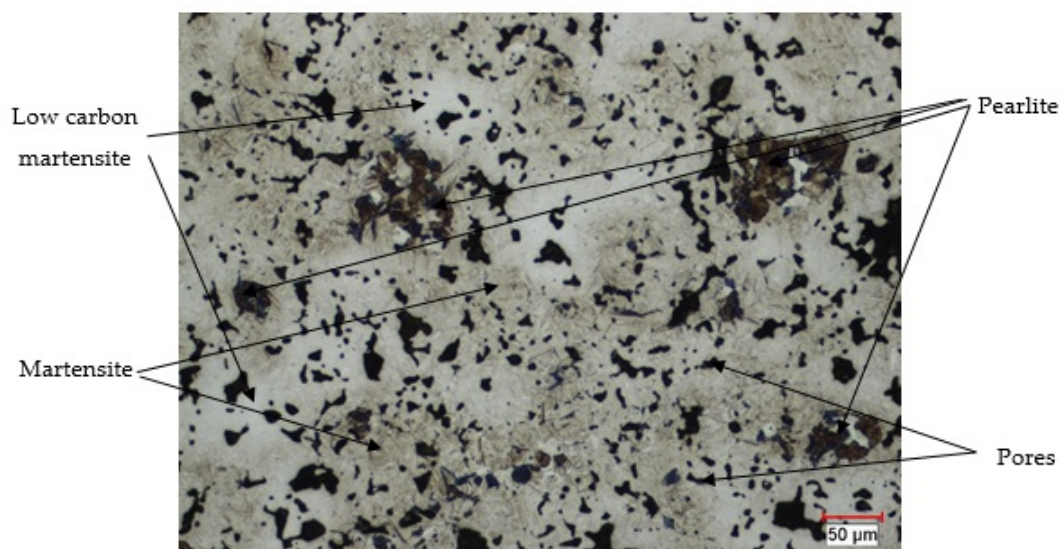


Figure 12. Optical image for sintered and heat treated bar, in the core region, prepared using powder mixture A' using magnification 200×.

The microstructure of the specimens produced from different powder mixtures, are presented in Figures 13–15. In this study, optical images at the core and surface regions were taken from each sample at magnification 200× for analysis.

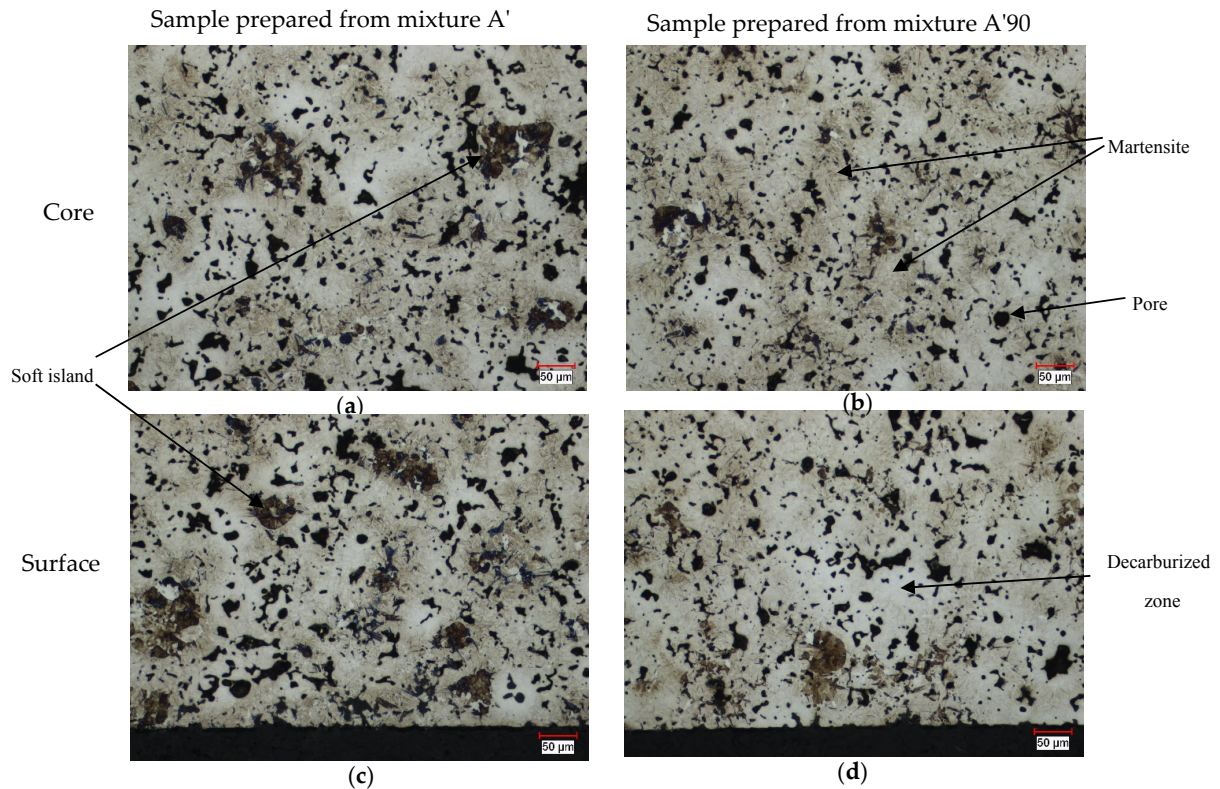


Figure 13. Optical images for sintered and heat treated bars prepared from powder mixtures A' and A'90 using magnification 200×, images (a,c) are for a sample prepared from mixture A' at core and surface, images (b,d) are for a sample prepared from mixture A'90 at core and surface respectively.

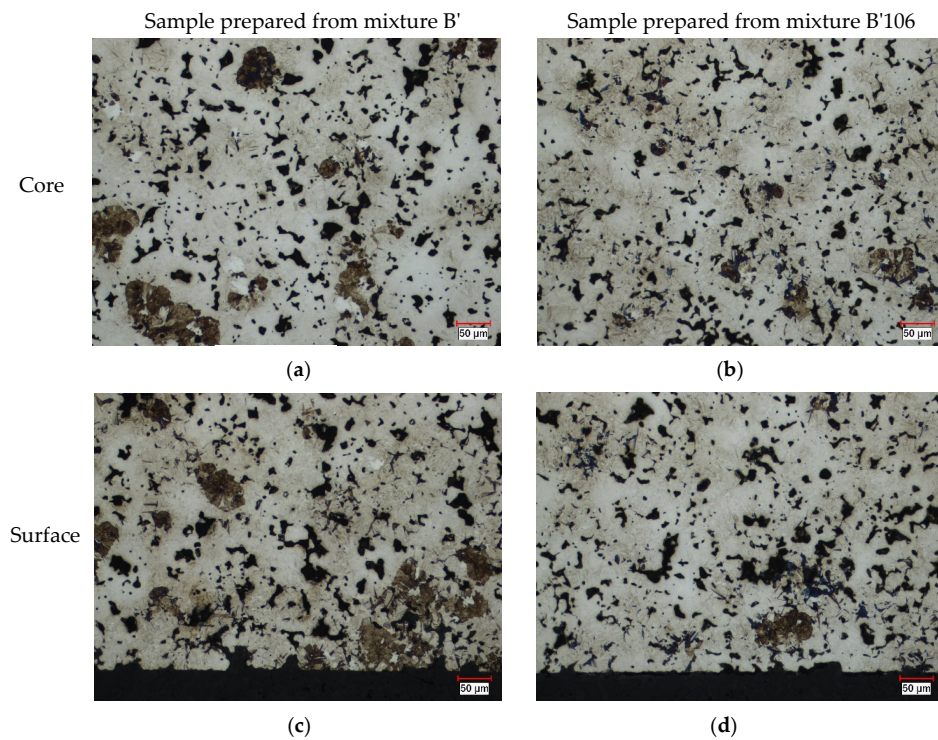


Figure 14. Optical images for sintered and heat treated bars prepared from powder mixtures B' and B'106 using magnification 200×, images (a,c) are for a sample prepared from mixture B' at core and surface, images (b,d) are for a sample prepared from mixture B'106 at core and surface respectively.

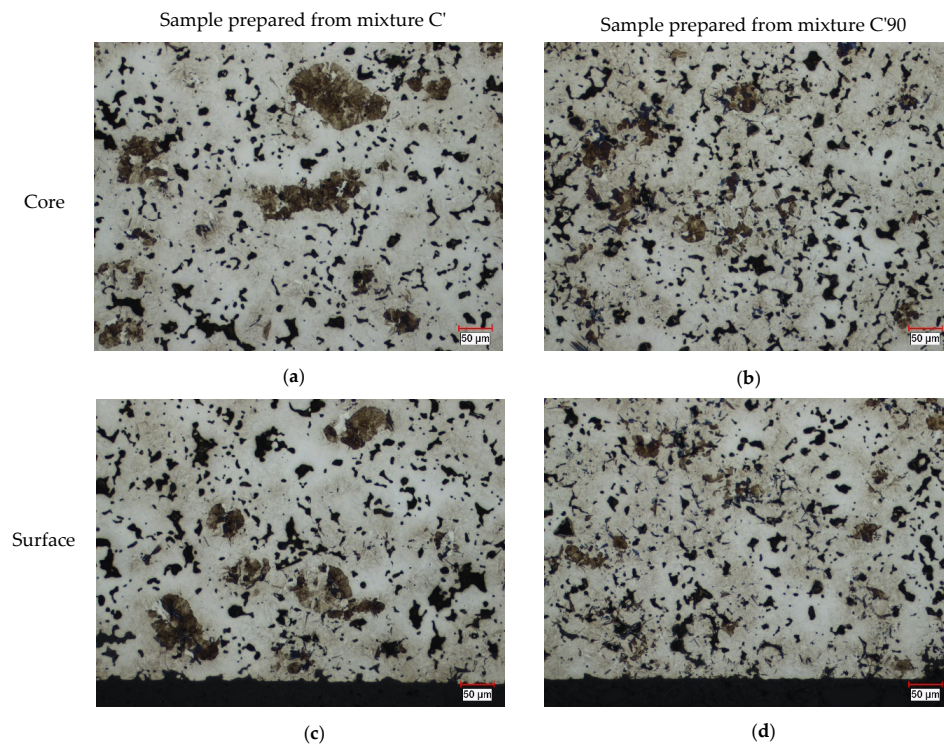


Figure 15. Optical images for sintered and heat treated bars prepared from powder mixtures C' and C'90 using magnification 200×, images (a,c) are for a sample prepared from mixture C' at core and surface, images (b,d) are for a sample prepared from mixture C'90 at core and surface respectively.

The study showed the presence of large islands of pearlite and low carbon martensite in the microstructure of samples prepared from mixtures containing iron powder in the as received state. While, the microstructure of samples prepared from mixtures containing sieved iron powder appeared to be mostly transformed to martensite at the core and surface regions. Decarburized zones were detected more clearly at the surface regions of all samples compared to the core regions due to carbon loss during sintering. Additionally, we could note a significant higher difference in the density of pearlitic islands on the core relative to surface regions due to the difference in the cooling rates.

4.4.3. Mechanical Properties of Sintered PMS

Transverse rupture strength was enhanced slightly with removing coarse iron particles from the powder mixtures, thus increasing the fraction of fine powder on the expense of coarse ones, as shown in Figure 16.

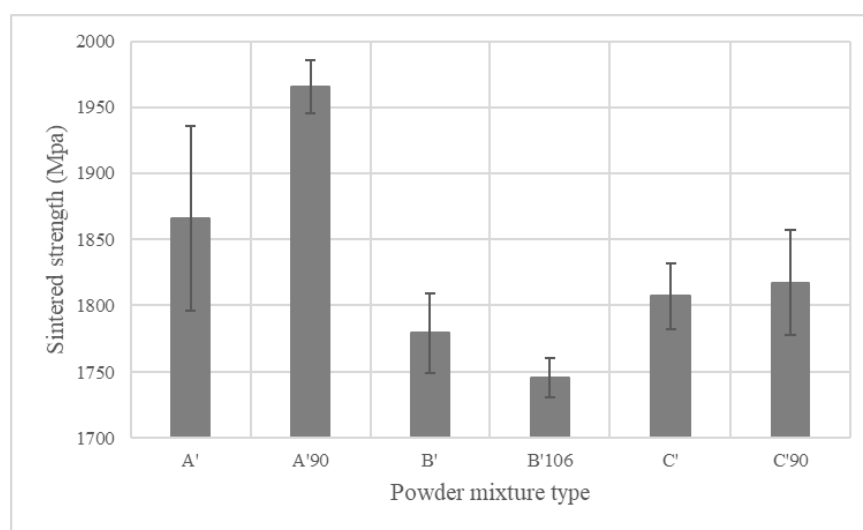


Figure 16. Sintered strength of standard TRS samples prepared from various PMS mixtures (including 0.7 wt. % of a lubricant).

This behavior was related to the increase in the surface area of the powder with narrowing particle size distribution by eliminating coarse particles, leading to the formation of stronger metallurgic bonds.

The apparent hardness (RHA) measured on the surface and core regions of a transverse cross section of the standard TRS samples in the sintered and heat treated state are shown in Figures 17 and 18. The obtained values of hardness for samples prepared from different mixtures were within the average of scatter of the measured values, and consequently no significant effect on hardness can be recognized with eliminating coarse particles.

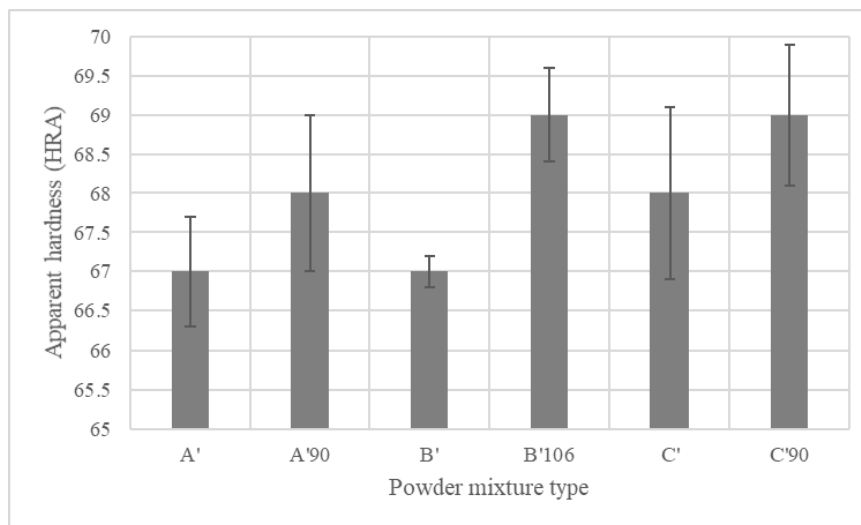


Figure 17. Apparent hardness for surface region of standard TRS samples prepared from various PMS mixtures (including 0.7 wt. % of a lubricant).

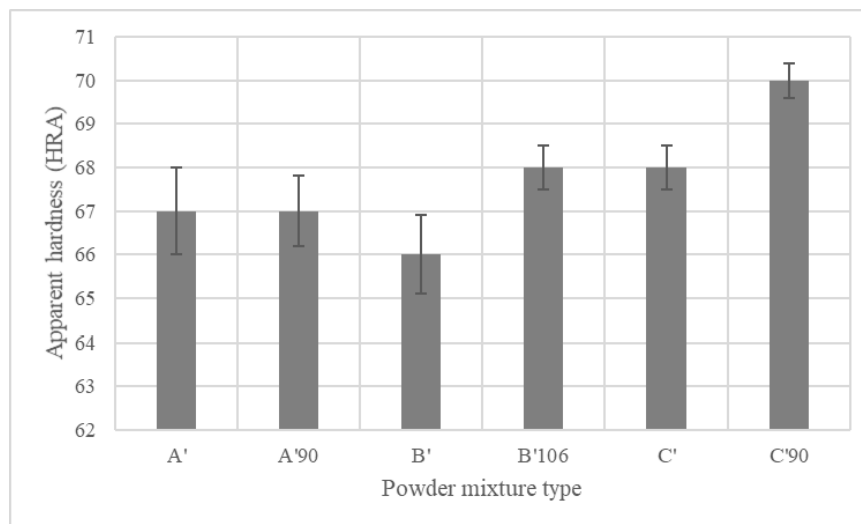


Figure 18. Apparent hardness for core region of standard TRS samples prepared from various PMS mixtures (including 0.7 wt. % of a lubricant).

5. Conclusions

In this study, three different types of Fe powders obtained from different manufactures were employed. For each type, the following sequence of actions was followed.

1. A histogram showing a size distribution was constructed.
2. Apparent density, flowability and compressibility were measured.
3. Particles whose sizes exceeded 180 μm were sieved away and the properties of the remaining powder were examined. Then particles with sizes greater than 150 μm were eliminated and the characteristics of the remaining powder were quantified.
4. Iterations continued until either flowability or compressibility became compromised by the described incremental removal of coarse particles. In other words, a threshold telling one when to stop taking away large particles was ascertained. According to experimental observations, the threshold was located within the 90–106 μm interval.
5. Iron powder from which particles with sizes exceeding the threshold were eliminated were then used for making a blend containing, in addition to Fe, Cr, Mo, Ni, graphite and a lubricant. Another

blend with an almost identical chemical composition was made of with-received (unsieved) Fe powder.

6. Both blends were compacted, sintered, austenitized and quenched. Then their microstructures and mechanical properties were compared.

It is not surprising that coarse particles were not properly alloyed during sintering and that, due to a reduced hardenability, they become pearlitic islands in the interior of the test bars. It is more surprising and much more important that their presence did not have a noticeable (statistically significant) adverse effect on the properties of PMS. This experimental observation (it was valid for all the three types of commercial Fe powders investigated), which was made for medium-density materials, suggests that it would be economically unfeasible to try to remove large particles from as-received powders, because gains in properties enhancement will be minimal. Such an indifference to the existence of large and soft inclusions can be explained if it is assumed that an initiation of cracks caused by an applied load happens at the pore/martensite rather than at the pearlite/martensite interface. Consequently, it can be contended that if the fraction of large pearlite colonies are such that an integrity, i.e., a 3D cohesiveness of the martensitic matrix, is not jeopardized, then they are not detrimental. It would be interesting to see whether the fraction can be estimated from the percolation theory, but such an explorative journey will be far beyond the scope of this contribution.

It must be admitted and accentuated that the conclusions are valid for a particular kind of PMS, which was specified in the introductory section. It is neither guaranteed nor even implied that they will remain defensible for high-density PMS whose fabrication may involve multiple stages including isostatic compression or for PMS, for which pre-alloyed iron is utilized instead of pure Fe.

It was convincingly shown by Danninger et al. [21] (1997 Danninger Spoljaric Weiss) that the presence of large and/or interconnected pores as initiators of cracks adversely affected the fatigue strength of powder metallurgy steels. A similar conclusion was arrived at by Beiss and Dalgic [22] (2001 Beiss Dalgic) who stated that an initiation of cracks in fatigue testing is localized on “few large irregular pores”. While it would be unjustified to dismiss the usefulness of tensile and hardness measurements, it should be acknowledged that by augmenting them with an investigation of such tribological characteristics as fatigue and creep strength, a deeper understanding of what coarse particles actually do to PM steels will be gained. Specifically, it can be investigated whether a mechanism of worsening of the fatigue strength due to their presence resembles that caused by large pores. Such an exploration was beyond the scope of this work.

Author Contributions: Conceptualization: D.V.M.; formal analysis: A.A., M.H.-K., D.V.M.; Investigation: A.A., M.H.-K., D.V.M.; Writing—original draft preparation: A.A.; Writing—review and editing: D.V.M.; Supervision: D.V.M. All authors have read and agreed to the published version of the manuscript.

Funding: This research was funded by Ontario Centre of Excellence.

Acknowledgments: The authors are grateful to Fanny Poon and Yannic Praden for technical assistance.

Conflicts of Interest: The authors declare no conflict of interest.

References

1. Poquillon, D.; Lemaitre, J.; Baco-Carles, V.; Tailhades, P.; Lacaze, J. Cold compaction of iron powders-relations between powder morphology and mechanical properties Part I: Powder preparation and compaction. *Powder Technol.* **2002**, *126*, 65–74. [[CrossRef](#)]
2. Sanchez, F.; Bolarin, A.M.; Molera, P.; Mendoza, J.E.; Ocampo, M. Relationship between particle size and manufacturing processing and sintered characteristics of iron powders. *Revista Latinoamericana de Metalurgia y Materiales* **2003**, *23*, 35–40.
3. Shima, S.; Saleh, M.A.E. The effect of particle characteristics on compaction behaviour of powders-Experiments. In Proceedings of the Powder Metallurgy World Congress, Kyoto, Japan, 12–15 July 1993; Part 1. pp. 331–334.

4. Tikhonov, G.F.; Sorokin, V.K. Theory, production technology and properties of powders and fibers-Effect of particle size distribution on technological properties of stainless steel powder. *Poroshkovaya Metallurgiya* **1971**, *10*, 1–4.
5. Peterson, J.E.; Small, W.M. Physical behavior of water atomized iron powders-Effects of relative humidity and particle size. *Int. J. Powder Metall.* **1993**, *29*, 121–130.
6. Peterson, J.E.; Small, W.M. Physical behavior of water atomized iron powders-Particle size distribution and apparent density. *Int. J. Powder Metall.* **1993**, *29*, 131–137.
7. Moon, L.H.; Kim, K.H. Relationship between compacting pressure, green density and green strength of copper powder compacts. *Int. J. Powder Metall.* **1984**, *27*, 80–84. [[CrossRef](#)]
8. Tallon, P.G. An Experimental Investigation of the Hardenability, Tensile and Fracture Properties of Powdered Metal Steels. Master's Thesis, McMaster University, Hamilton, ON, Canada, 26 April 2018.
9. Suh, S.; Patel, S.; Nash, P. A study of compressibility, green and sintered strength of iron powders. In Proceedings of the 1991 Powder Metallurgy Conference and Exhibition, Chicago, IL, USA, 9–12 June 1991; Volume 5, pp. 151–160.
10. Zhorniyak, A.F.; Oliker, V.E. Effect of the particle size distribution of atomized iron powder and mixtures of atomized and reduced iron powders on some properties of materials produced from them by pressing and sintering. *Poroshkovaya Metallurgiya* **1978**, *17*, 558–561. [[CrossRef](#)]
11. Oikonomou, C.; Hryha, E.; Nyborg, L.; Ahlin, Å. Effect of powder properties on the compressibility of water atomized iron and low alloyed steel grades. In Proceedings of the Euro PM, Gothenburg, Sweden, 15–18 September 2013.
12. Sanchez, F.; Bolarin, A.M.; Coreno, J.; Mendoza, J.E.; Bas, J.A. Effect of compaction process sequence on axial density distribution of green compacts. *Int. J. Powder Metall.* **2001**, *44*, 351–354. [[CrossRef](#)]
13. Sorokin, V.K. Compressibility of stainless-steel powder. *Poroshkovaya Metallurgiya* **1968**, *10*, 22–26.
14. Fischmeister, H.F.; Arzt, E.; Olsson, L.R. Particle deformation and sliding during compaction of spherical powders: A study by quantitative metallography. *Powder Metall.* **1978**, *21*, 179–181. [[CrossRef](#)]
15. Fischmeister, H.F.; Arzt, E. Densification of powders by particle deformation. *Powder Metall.* **1983**, *26*, 82–88. [[CrossRef](#)]
16. Kiparisov, S.S.; Panov, V.S.; Smirnova, M.M.; Kots, Y.F. Properties of steel powders of various particle size and the structure of the steel in the sintered condition. *Poroshkovaya Metallurgiya* **1981**, *6*, 9–15. [[CrossRef](#)]
17. Lund, J.A. Origins of green strength in Iron P/M compacts. *Int. J. Powder Metall.* **1982**, *18*, 117–127.
18. Jackson, J.G.; Ehrgott, J.Q.; Rohani, B. Loading rate effects on compressibility of sands. *J. Geotech. Eng. Div.* **1980**, *106*, 839–852.
19. Barr, A.D.; Clarke, S.D.; Petkovski, M.; Tyas, A.; Rigby, S.E.; Warren, J.; Kerr, S. Effects of strain rate and moisture content on the behaviour of sand under one-dimensional compression. *Exp. Mech.* **2016**, *56*, 1625–1639. [[CrossRef](#)]
20. German, R.M. *Powder Metallurgy Science*; MPIF: Princeton, NJ, USA, 1994.
21. Danninger, H.; Spoljaric, D.; Weiss, B. Microstructural features limiting the performance of P/M steels. *Int. J. Powder Metall.* **1997**, *33*, 43–53.
22. Beiss, P.; Dalgic, M. Structure property relationships in porous sintered steels. *Mater. Chem. Phys.* **2001**, *67*, 37–42. [[CrossRef](#)]

